

Supporting Information For

***De novo* structure prediction and experimental characterization of folded peptoid oligomers**

Glenn L. Butterfoss^{1*}, Barney Yoo^{2*}, Jonathan N. Jaworski^{3†}, Ilya Chorny⁴, Ken A. Dill^{5‡}, Ronald N. Zuckermann³, Richard Bonneau¹, Kent Kirshenbaum², Vincent A. Voelz^{6‡}

¹New York University, Center for Genomics and Systems Biology, NY, New York 10003, USA; ²New York University, Dept. of Chemistry, NY, New York 10003, USA; ³Molecular Foundry, Lawrence Berkeley National Laboratory, 1 Cyclotron Rd., Berkeley, CA 94720, USA; ⁴Simprota Corporation, San Francisco, CA; ⁵Laufer Center for Physical and Quantitative Biology, Stony Brook University, NY; ⁶Temple University, Dept. of Chemistry, Philadelphia, PA

*These authors contributed equally to this work.

†present address: Dept. of Chemistry, University of Wisconsin, Madison, WI 53706

‡corresponding authors

Supporting Figures	3
Figure S1. Crystal structure of H-(Npe) ₃ -OH.	3
Figure S2. Crystal structure of cyclo-(Nspe) ₉	4
Table S1. Dunitz nitrogen pyramidalization (χ_N), carbon pyramidalization (χ_C), and amide twist (T) parameters for the crystal structure of cyclo-(Nspe) ₉	5
Figure S3. QM calculations suggest a steric clash may be responsible for amide non-planarity of residue 5.	6
Figure S4. Potentials of mean force and probability distributions for backbone ω angles and Dunitz χ_N parameters.	7
Figure S5. ¹ H-NMR of cyclo-(Nspe) ₉ in CDCl ₃	8
Figure S6. ¹ H- ¹³ C-HSQC of cyclo-(Nspe) ₉ in CDCl ₃	9
Figure S7. 2D-COSY spectra of cyclo-(Nspe) ₉ in CDCl ₃	10
Figure S8. Circular dichroism spectra of cyclo-(Nspe) ₉	10
Figure S9. A funnel-like conformational free energy landscape of cyclo-(Nspe) ₉ , predicted by REMD.	11
Figure S10. Backbone-RMSD distributions for conformational ensembles of peptoid targets sampled by REMD.	12
Supporting Materials and Methods	13
Peptoid synthesis and purification.	13
Conformational free energy calculations for <i>N</i> -aryl and <i>N</i> -alkyl peptoid trimers	14
Figure S11. Definitions of dihedral angles used in the conformational analysis of <i>N</i> -aryl peptoid trimer 1 and <i>N</i> -alkyl peptoid trimer 2.	15
Selection of predicted structures for <i>N</i>-aryl and <i>N</i>-alkyl peptoid trimers	16
Table S2. The 15 lowest-free energy torsion states for <i>N</i> -aryl trimer 1.	17
Figure S12. Submitted lowest-free energy structures for <i>N</i> -aryl trimer 1.	17
Table S4. The 16 lowest-free energy torsion states for <i>N</i> -alkyl trimer 2.	19
Figure S13. Structures of submitted predictions for the <i>N</i> -alkyl peptoid trimer 2.	19
Table S5. QM optimizations of various trimer 2 conformations.	20
Figure S14. Selected structures of optimized trimer 2 conformations.	20
Conformational free energy calculations for the cyclic peptoid nonamer	21

Table S6. Free energies of <i>cis/trans</i> states of cyclo-(Nspe) ₉ , as predicted from restrained and unrestrained REMD simulations.....	21
Table S7. The ranked list of (omega-phi) torsional state free energies predicted by (unrestrained) REMD simulation.	22
<i>Ab initio</i> refinement and prediction selection for the cyclic peptoid nonamer.....	23
Table S8. Single-point <i>ab initio</i> QM energies of cyclo-(Nspe) ₉ conformations selected from REMD simulations, calculated using various model chemistries.	24
Figure S15. Conformational clusters of cyclo-(Nspe) ₉ , ranked by (top) B3LYP/6-31G*** and (bottom) M05-2X/6-311G**.....	26
Table S9. A summary of the backbone structures of submitted structure predictions for cyclo-(Nspe) ₉	27
Figure S16. Conformational clusters corresponding to the three lowest-energy <i>cccctcct</i> states.	27
Figure S17. Conformational clusters corresponding to the lowest-energy states for states (a) <i>cccccttt</i> (b) <i>cccctcctt</i> and (c) <i>ccccccct</i>	28
QM calculations comparing experimental and predicted structures	28
Table S10. Relative energies (kcal/mol) of cyclo-(Nspe) ₉ after optimization at HF/3-21G* without ethanol	28
What are the effects of Nspe side chains?	29
Table S11. Relative energies (kcal/mol) of cyclo-(Sar) ₉ after optimization at HF/3-21G* without ethanol	29
What is the effect of ethanol?	29
Table S12. Relative energies (kcal/mol) of cyclo-(Sar) ₉ after optimization at HF/3-21G* with ethanol. Energies are then calculated with (+) or without (-) the ethanol	29
Table S13. RMSD of optimized structures in this section, compared to the experimental crystal structure using backbone C α , N, C, and O:	30
References.....	30

Supporting Figures

Figure S1. Crystal structure of H-(Npe)₃-OH.

Eight monomers of H-(Npe)₃-OH fill the crystal structure unit cell as asymmetric units. Hydrophobic/polar partitioning can be seen as distinct layers in the crystal lattice. The view of the unit cell is down the *b*-axis, visualized using EnCIFer.

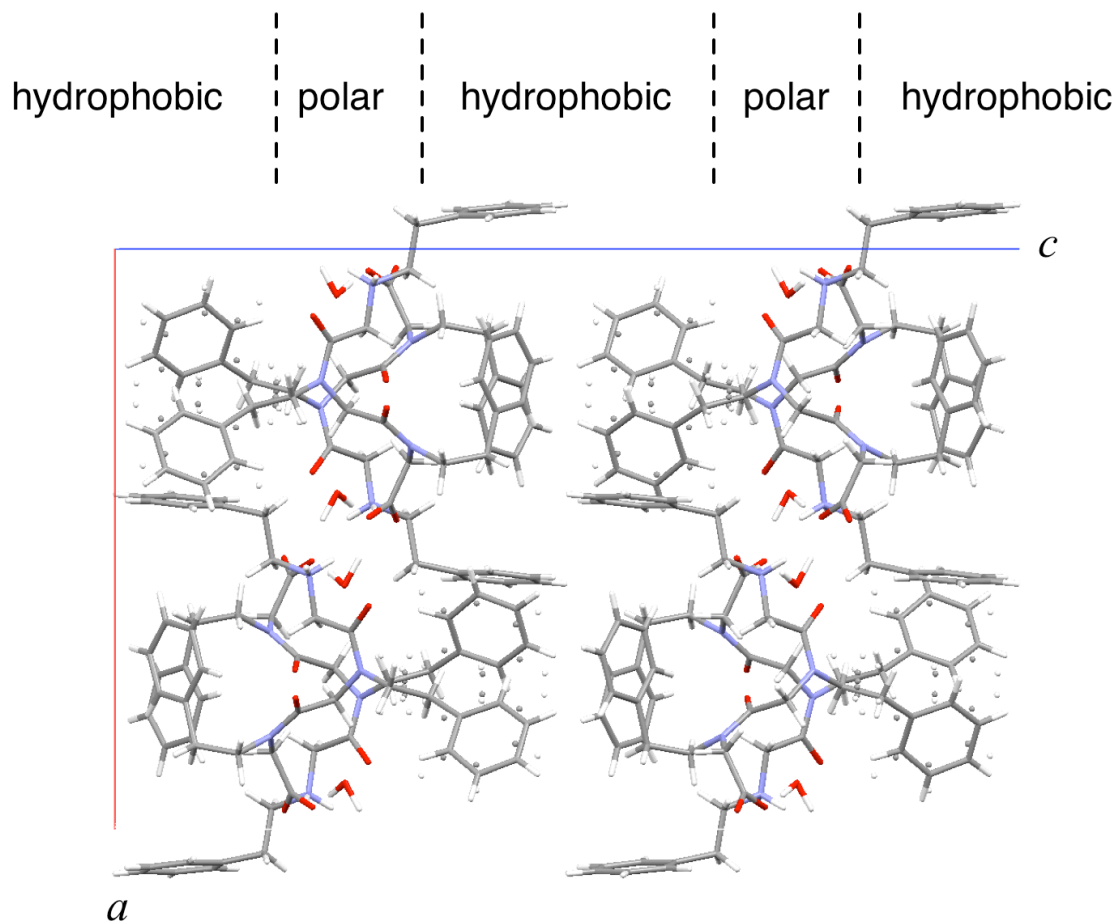


Figure S2. Crystal structure of cyclo-(Nspe)₉.

(a) Top view; (b) backbone displaying *cis* (c) and *trans* (t) amide bonds; (c) side view. Intermolecular packing is attained primarily through side chain phenyl-phenyl contacts, as well as bound ethanol molecules which are stabilized by favorable hydrogen bonding between ethanol hydroxyl groups and backbone carbonyls.

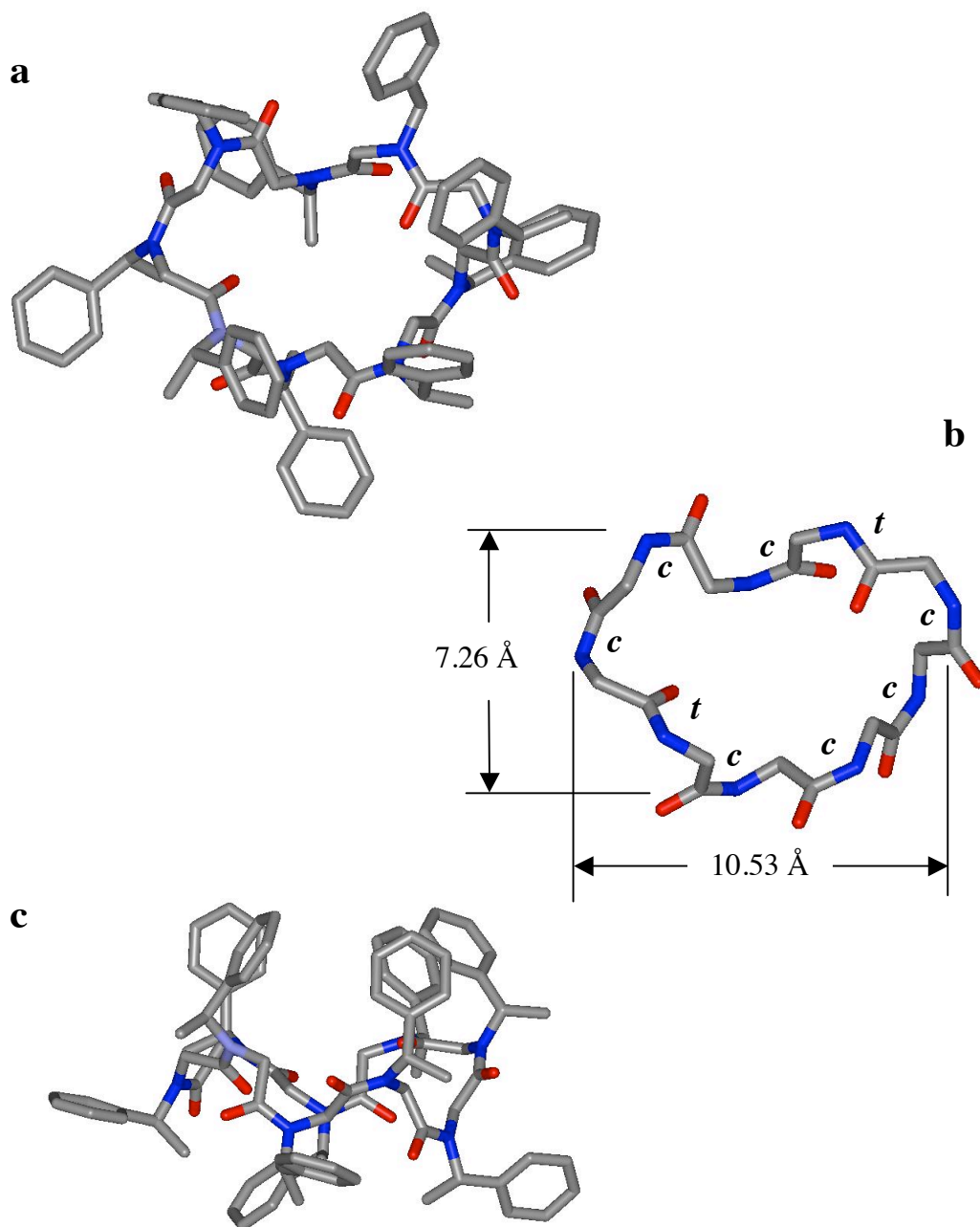


Table S1. Dunitz nitrogen pyramidalization (χ_N), carbon pyramidalization (χ_C), and amide twist (T) parameters for the crystal structure of cyclo-(Nspe)₉.

Parameters are defined by Winkler and Dunitz (1) as $\chi_N = \omega_2 - \omega_3 + 180$, $\chi_C = \omega_1 - \omega_3 + 180$, where $\omega_1 = \angle(C\alpha_i - C_i - N_{i+1} - C\alpha_{i+1})$, $\omega_2 = \angle(O_i - C_i - N_{i+1} - NC\alpha_{i+1})$, $\omega_3 = \angle(O_i - C_i - N_{i+1} - C\alpha_{i+1})$, and $\angle(C\alpha_i - C_i - N_{i+1} - NC\alpha_{i+1})$. All angles are in degrees.

residue	χ_N	χ_C	T	T (deviation)*
1	-7.77	-0.74	-5.83	5.83
2	1.25	1.14	4.06	4.06
3	20.95	3.27	0.78	0.78
4	1.27	-1.05	-3.55	3.55
5	16.08	6.93	162.94	17.06
6	13.33	-1.56	-7.13	7.13
7	5.06	-3.37	-1.20	1.20
8	17.75	-1.95	-3.78	3.78
9	6.43	1.10	174.40	5.60

* deviation of T from from ideal values

Figure S3. QM calculations suggest a steric clash may be responsible for amide non-planarity of residue 5.

QM studies of cyclo-(sarcosine)₉ suggest the amide backbone deviations from planarity ($\omega_5 = 151.5^\circ$) seen in for residue 5 in the crystal structure of cyclic peptoid **3** may be facilitated by a steric clash between the amide oxygen and (*i*-2) H α atom. (Top) A cyclo-(sarcosine)₉ analog of the crystal structure of **3**, shown with the relevant steric interaction (dotted line) and ω_5 dihedral angle. (Bottom) Cyclo-(sarcosine)₉ conformations optimized at the HF/3-21G* level of theory starting from the crystal backbone, for various fixed values of ω_5 , show large increases in energy (squares) as the H-O distance (filled circles) decreases.

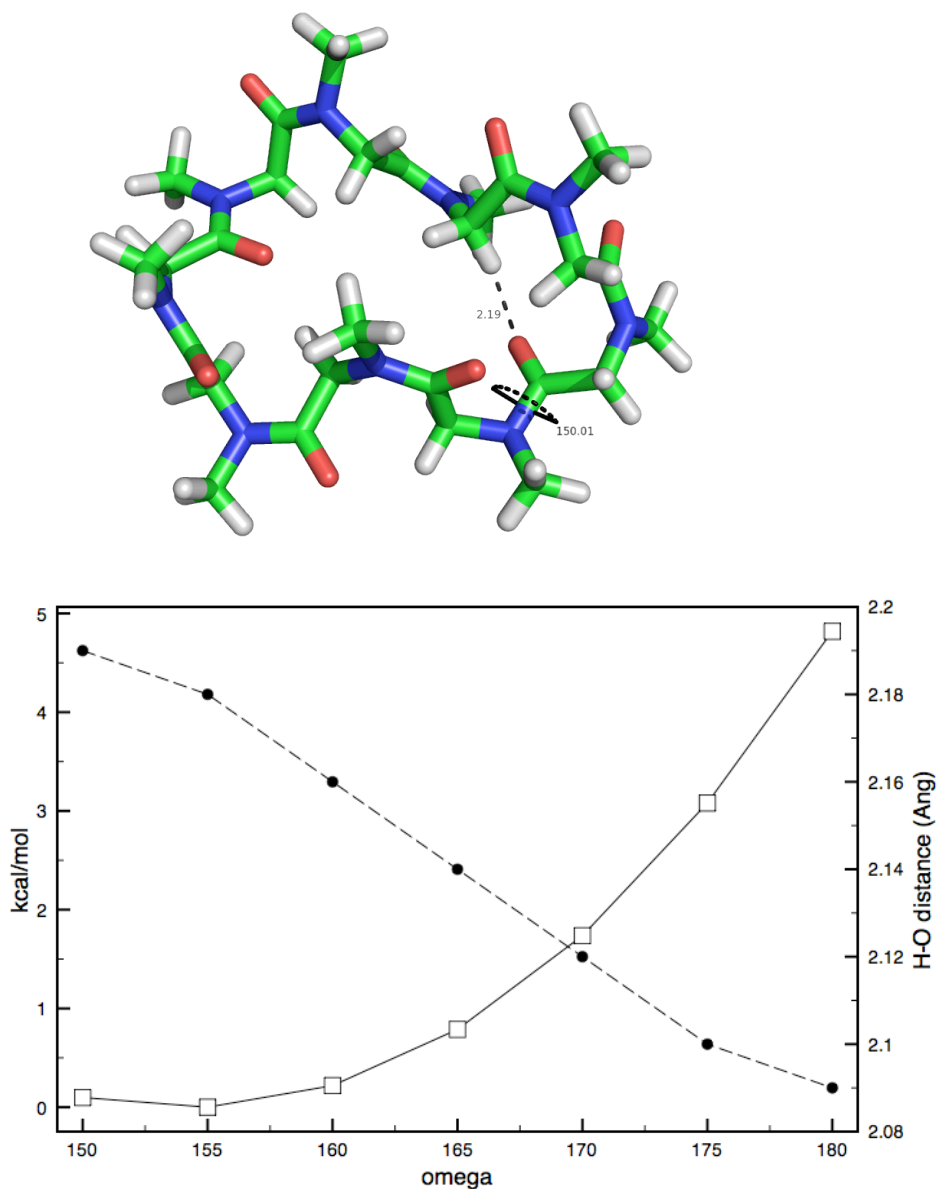


Figure S4. Potentials of mean force and probability distributions for backbone ω angles and Dunitz χ_N parameters.

(a) PMF(ω) and (b) $P(\omega)$ for cyclo-(Nspe)₉ (peptoid **3**) calculated from the REMD simulations, show a region of increased probability at ω angles near $\sim 150^\circ$, as seen in the crystal structure for residue 5. Plots are annotated with ω angles seen in the crystal structure, labeled by residue number. Error bars represent uncertainty in free energies calculated across all residues. (c) PMF(χ_N) and (d) $P(\chi_N)$ for cyclo-(Nspe)₉, labeled as in (a) and (b). (See Table S1 for the definition of the Dunitz χ_N parameter.)

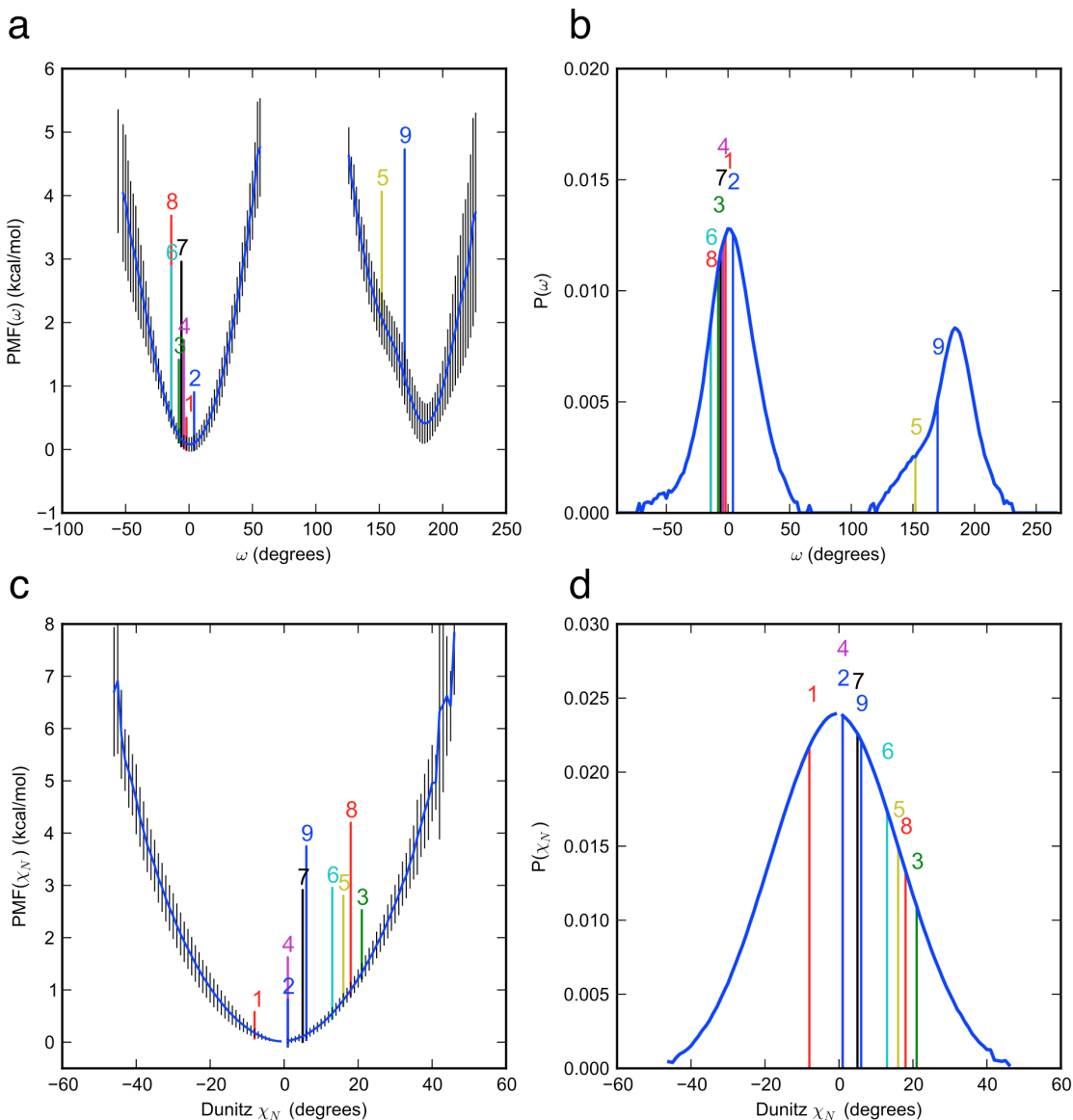


Figure S5. $^1\text{H-NMR}$ of cyclo-(Nspe) $_9$ in CDCl_3 .

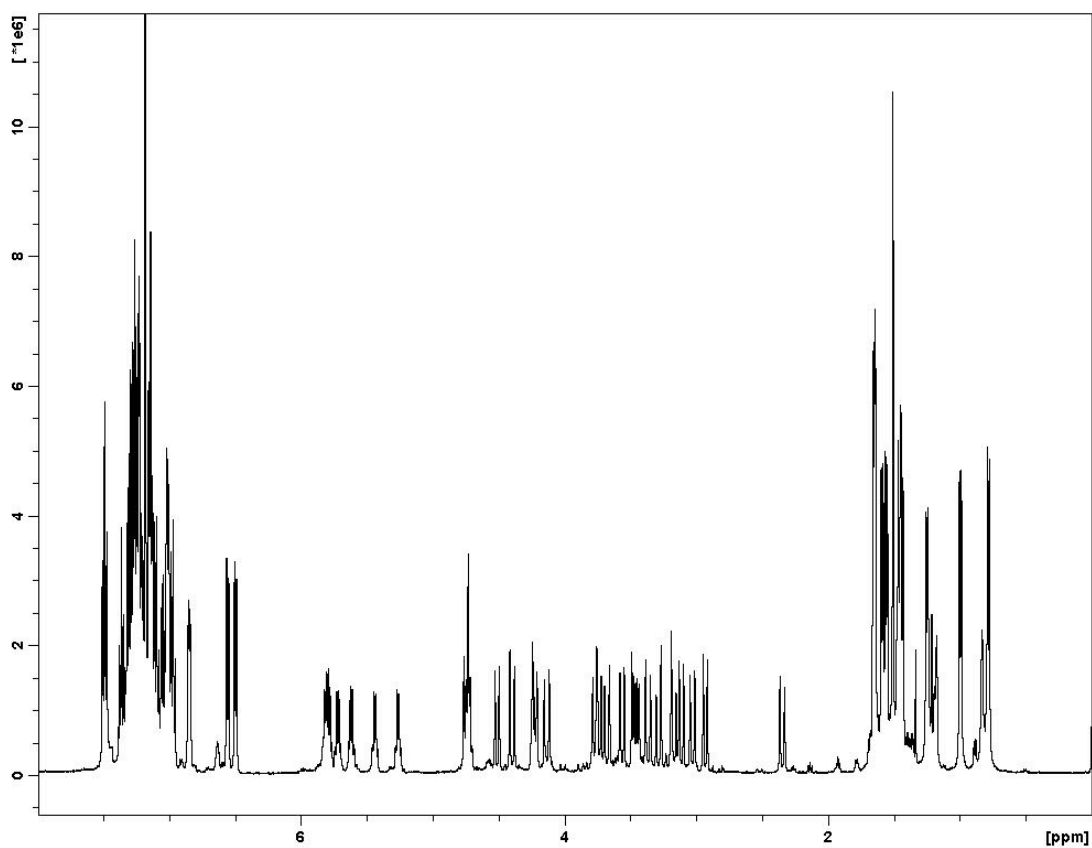
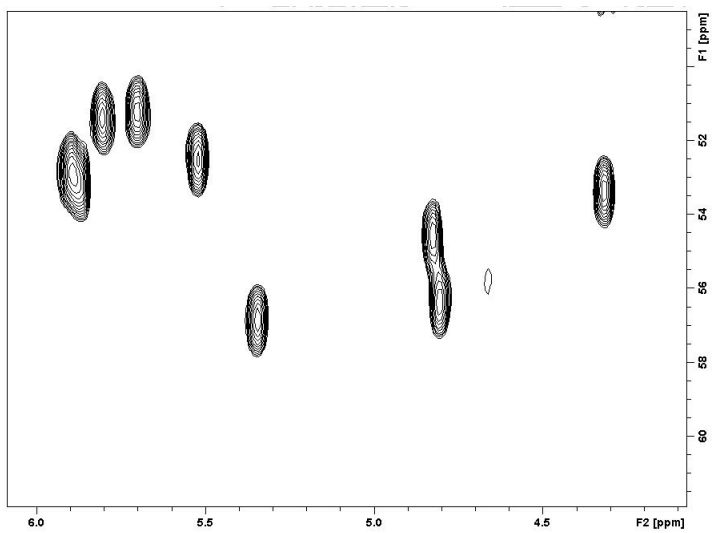
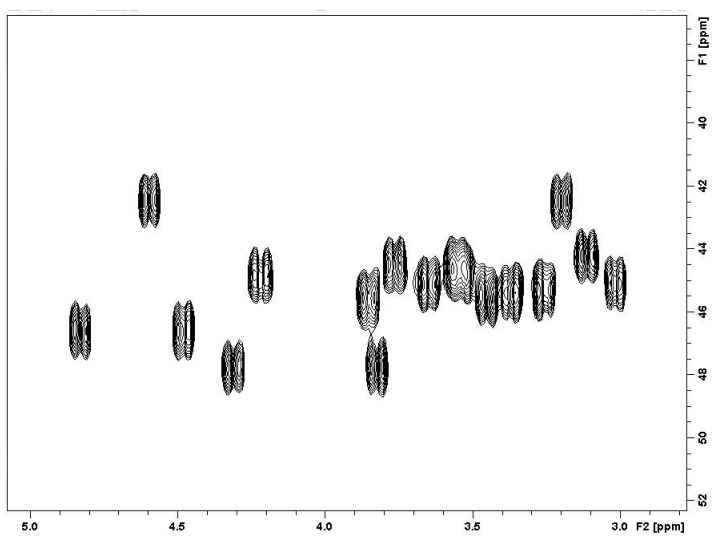


Figure S6. ^1H - ^{13}C -HSQC of cyclo-(Nspe) $_9$ in CDCl_3 .



Nine side chain methine groups



18 backbone methylene groups

Figure S7. 2D-COSY spectra of cyclo-(Nspe)₉ in CDCl₃.

The backbone methylene proton correlations are shown. Nine off diagonals are observed.

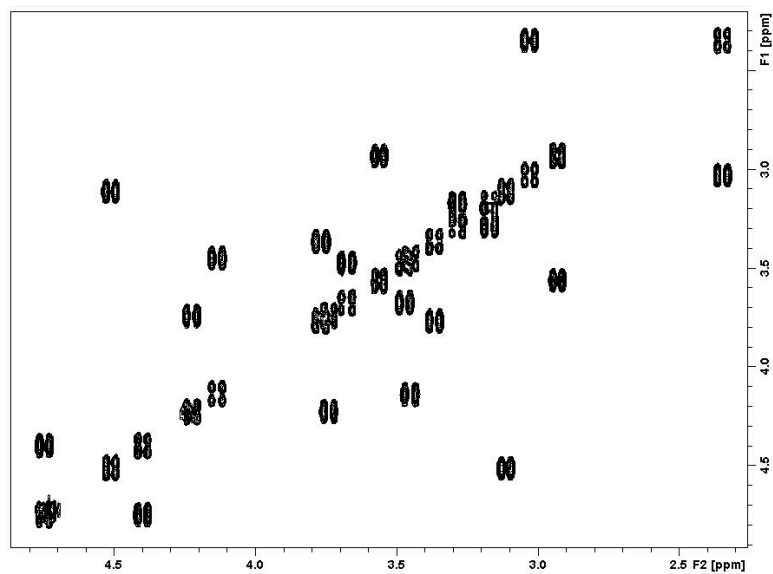


Figure S8. Circular dichroism spectra of cyclo-(Nspe)₉.

Peptoid concentrations were ~50 μ M in methanol.

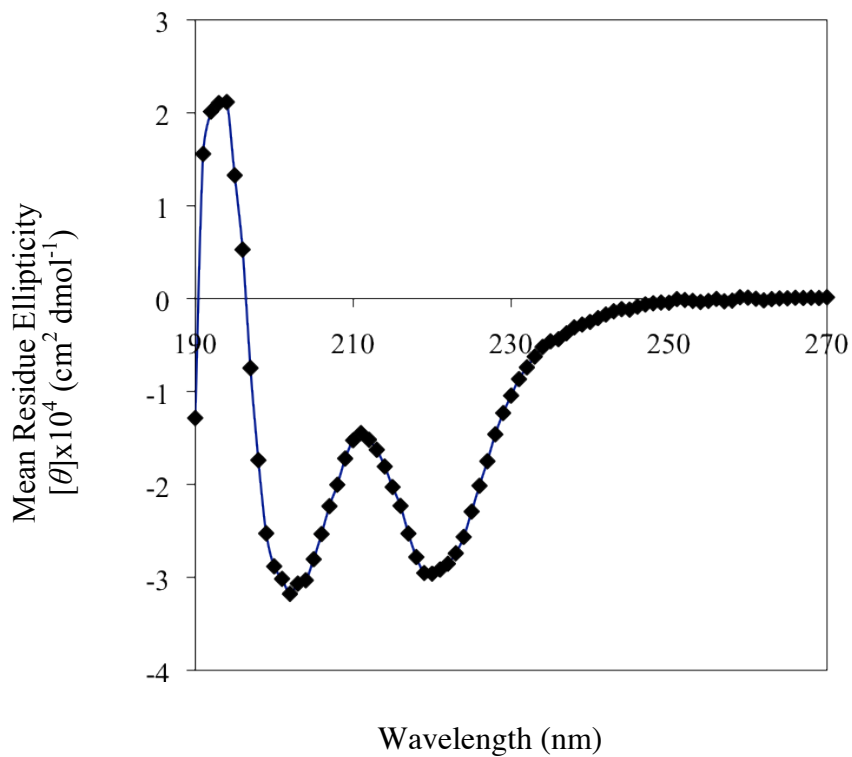


Figure S9. A funnel-like conformational free energy landscape of cyclo-(Nspe)₉ predicted by REMD.

Marked by arrows are the relative REMD ranks of *pick1*, our top-ranked (QM-refined) submitted prediction (yellow, ~1.22 kcal/mol), and the experimental crystal structure (cyan, ~3.08 kcal/mol).

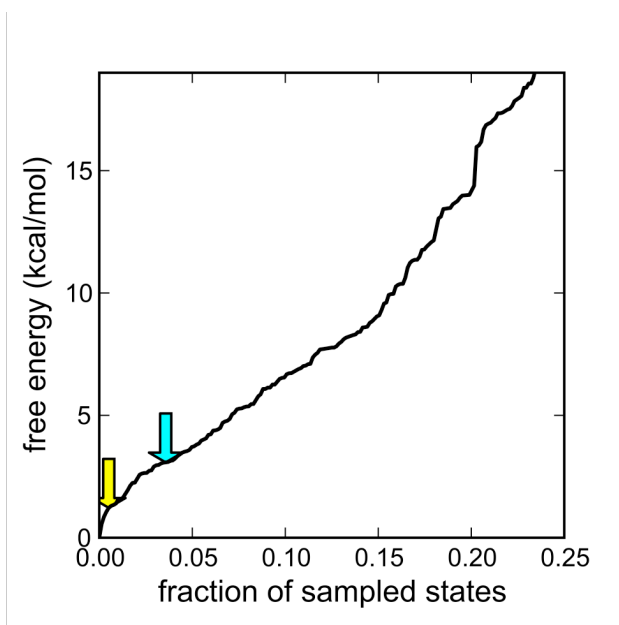
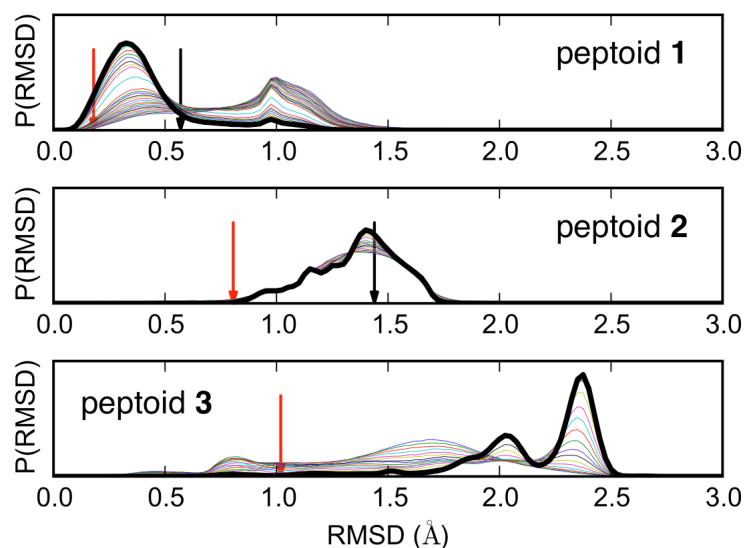


Figure S10. Backbone-RMSD distributions for conformational ensembles of peptoid targets sampled by REMD.

The thick black line represents the lowest-temperature replica (300K), and the thin colored lines denote higher temperature replicas (up to 800K). Black arrows denote RMSD-backbone values of minimized low-energy structures taken the torsional state with the lowest free energy (i.e. our top predictions from REMD simulations). Red arrows denote RMSD-backbone values for the lowest-energy structures obtained by QM refinement (i.e. our best predictions).



Supporting Materials and Methods

Peptoid synthesis and purification.

All reactions were conducted at room temperature. 200 mg of 2-chlorotrityl chloride resin was washed twice in 2 mL of DCM, followed by swelling in 2 mL of DCM. The first monomer was introduced manually by reacting 45 mg of bromoacetic acid (0.33 mmol; Sigma-Aldrich) and 189 μ L of DIEA (1.08 mmol; Chem Impex International) in 5 mL of DCM on a shaker platform for 30 minutes, followed by five 2 mL washes with DCM and DMF. The bromoacylated resin was incubated with 2 mL of 1 M amine submonomer in DMF on a shaker platform for 30 minutes at room temperature, followed by extensive washes with DMF (five times with 2 mL). After manual loading of the first monomer, the eight subsequent bromoacetylation and amine displacement steps were performed on the robotic synthesizer. The automated bromoacetylation step was performed by adding 1 mL of 0.6 M of DIC (Chem Impex International) and 1 mL of 0.6 M bromoacetic acid in DMF. The mixture was agitated for 30 min, drained, followed by three 2 mL washes with DMF. Next, 2 mL of a 1 M solution of submonomer (2 mmol) in DMF was added to introduce the side chain by nucleophilic displacement of bromide. The mixture was agitated for 30 min, drained, washed with DMF (three times with 2 mL) and washed with DMF (three times with 2 mL). The peptoid-resin was cleaved with a 2 mL solution of 20% HFIP (Alfa Aesar) in DCM (v/v). The cleavage was conducted in a glass tube with constant agitation for 30 minutes. HFIP/DCM was evaporated using a rotary evaporator. The final product was dissolved in 5 mL of 50% ACN in HPLC grade H₂O and filtered with a 0.5 μ m stainless steel fritted syringe tip filter (Upchurch Scientific). The linear (Nspe)₉ were analyzed on a C18 reversed-phase analytical RP-HPLC column at room temperature (Peeke Scientific, 5 μ m, 120 Å, 2.0 x 50 mm) using a Beckman Coulter System Gold instrument. A linear gradient of 5–95% acetonitrile/water (0.1% TFA, Acros Organics) over 20 min was used with a flow rate of 0.7 mL/min. Preparative HPLC was performed on a Delta-Pak C18 (Waters, 15 μ m, 100 Å, 25 x 100mm) with a linear gradient of 5–95% acetonitrile/water (0.1% TFA) over 60 min with a flow rate of 5 mL/min. LCMS was performed on an Agilent 1100 Series LC/MSD Trap XCT (Agilent Technologies). To obtain cyclo-(Nspe)₉, 30 μ moles of the purified linear oligomer was suspended in 5 mL of DMF; followed by the addition of PyBOP (45 mg in 1 mL DMF) and DIEA (45 μ L in 1mL DMF). The reaction was allowed to proceed for 5 minutes at room temperature. Crude cyclo-(Nspe)₉ was purified by preparative HPLC as described above.

Conformational free energy calculations for *N*-aryl and *N*-alkyl peptoid trimers

REMD calculations used the ZAM algorithm (2, 3) to spawn and manage AMBER simulations for each replica over Linux cluster nodes. In REMD, simulation replicas at different temperatures are exchanged according a Metropolis criterion at regular intervals. Data generated from the generalized ensemble can be reweighted to compute observables at any temperature. The last half of the REMD trajectories were used for analysis. Conformational free energies were calculated from the ten lowest-temperature replicas, using the Multistate Bennett Acceptance Ratio (MBAR) method (4) (see Methods).

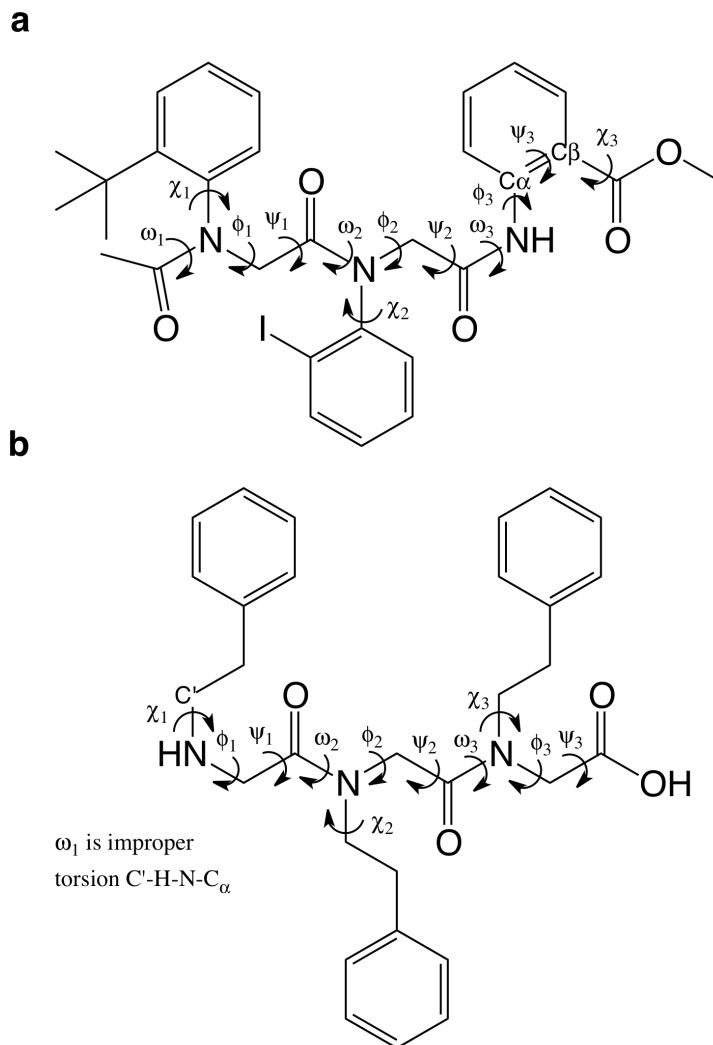
For the purposes of selecting peptoid conformations in our structure prediction efforts, we considered the set of all possible backbone torsion states to be states, each defined by the $(\omega_i, \phi_i, \psi_i)$ dihedral angles for each peptoid residue i (**Figure S1**). Conformations were binned into discrete states according to a set of a binary classifications: the ω angle defined either a *cis* ($-90^\circ < \omega \leq +90^\circ$) or *trans* ($90^\circ < \omega \leq +270^\circ$) backbone amine; the ϕ -angle was either be positive ($\phi > 0^\circ$) or negative ($\phi \leq 0^\circ$); the ψ -angle state was either in the α_D or $C_{7\beta}$ dihedral minima (defined as the nearest minima in (ϕ, ψ) space, where $\alpha_D = (\pm 90^\circ, 180^\circ)$ and $C_{7\beta} = (-120^\circ, 75^\circ)$ or $(120^\circ, -75^\circ)$). (For a more complete discussion of these dihedral minima, please see Butterfoss et al. (5))

Some of these angle definitions (ψ_3 in molecule **1**, ω_1 in molecule **2**) are non-informative but were defined out of convenience to work with our analysis scripts. Using these state definitions, the total number of possible torsion states is $2^9 = 512$. We find that about half of the possible torsion states (~ 250) are actually sampled at low temperatures (below 490K). Although mirror-image conformational states are considered as unique states in this analysis, we combine these states when the selecting structures for further analysis (see below).

For the purpose of computing conformational free energy landscapes of each trimer, we considered torsional states defined by $(\omega_i, \phi_i, \psi_i, \chi_i)$ dihedral angles for each peptoid residue i (**Figure S1**), where an additional binary classification of positive ($\chi > 0^\circ$) or negative ($\chi \leq 0^\circ$) is used for the χ -angle. Despite the additional structural resolution, we still find that ~ 250 states are sampled at low temperatures. Interestingly, for the *N*-aryl trimer **1**, we sample only negative χ angles in the REMD simulations for the ortho-iodo-substituted *N*-aryl peptoid residue, consistent with experimental findings that isomerization of this group is extremely slow for peptoid **1**. Nevertheless we can estimate the free energies of the major (negative χ -angle) and minor (positive χ -angle) conformers seen in the crystal structure of **1**, from mirror-image conformational states, which are sampled in the REMD simulations.

Figure S11. Definitions of dihedral angles used in the conformational analysis of *N*-aryl peptoid trimer **1 and *N*-alkyl peptoid trimer **2**.**

Note that ψ_3 for trimer **1** (N-C α -C β -C) and ω_1 for trimer **2** (improper torsion C'-H-N-C α) are non-physical, and defined for the convenience of our analysis scripts. Side chain dihedral angles χ_i are defined with respect to the carbonyl carbon of the preceding residue. Thus, for residue 1 of trimer **2**, we used the amine hydrogen as a proxy, defining χ_1 as the dihedral angle H-N-C1-C2, and ϕ_1 as the dihedral angle H-N-C α -C.



Selection of predicted structures for *N*-aryl and *N*-alkyl peptoid trimers

To select a finite set of conformations as our submitted predictions, we minimized the five lowest-energy snapshots observed for each torsional state, and used the lowest-energy structures as our submitted predictions. The ranking of these predictions were by lowest conformational free energy. Different conformational states often minimized to the same basin of structures (for instance, ψ -angles corresponding to the α_D versus $C_{7\beta}$ state were actually one conformational basin). In these cases, we grouped together the conformational states together for ranking. Mirror-image conformational basins were also grouped together for ranking.

For each conformational (torsion) state, we calculated average energy; the minimum energy sampled by REMD; and the lowest energy obtained after minimizing the 5 lowest-energy snapshots for each torsion state (**Table S2**). Note that the ranking of lowest minimized energies differs from the ranking of free energies. The final submitted predictions were six conformations from groups (a) through (f) (see **Table S2**, **Figure S12**).

Table S2. The 15 lowest-free energy torsion states for *N*-aryl trimer 1.

state	ΔG (kcal/mol)	$\langle E \rangle$ (kcal/mol)	Min(E) sampled (kcal/mol)	E after minimization (kcal/mol)	group	ω_1	ϕ_1	ψ_1	ω_2	ϕ_2	ψ_2	ω_3	ϕ_3	ψ_3
1	0.000	-14.442	-31.327	-64.069	a	trans	+	α_D	trans	+	$C_{7\beta}$	trans	-	α_D
2*	0.113	-14.434	-30.438	-64.178	a	trans	+	α_D	trans	+	$C_{7\beta}$	trans	-	$C_{7\beta}$
3	0.255	-13.708	-31.372	-63.168	a	trans	+	α_D	trans	+	α_D	trans	-	α_D
4	0.309	-13.552	-32.206	-64.05	a	trans	+	α_D	trans	+	α_D	trans	-	$C_{7\beta}$
5	0.380	-14.301	-30.720	-63.919	a	trans	+	α_D	trans	+	α_D	trans	+	α_D
6	0.563	-14.136	-29.332	-64.069	a	trans	+	α_D	trans	+	α_D	trans	+	$C_{7\beta}$
7	0.672	-13.227	-31.048	-61.905	b	trans	+	α_D	trans	+	$C_{7\beta}$	trans	+	α_D
8*	0.698	-13.092	-30.969	-62.352	b	trans	+	α_D	trans	+	$C_{7\beta}$	trans	+	$C_{7\beta}$
9	1.399	-12.842	-27.831	-59.898	c	trans	+	α_D	trans	-	$C_{7\beta}$	trans	-	$C_{7\beta}$
10*	1.412	-12.833	-28.709	-59.675	d	trans	+	α_D	trans	-	α_D	trans	+	$C_{7\beta}$
11	1.469	-12.797	-27.707	-58.857	c	trans	+	α_D	trans	-	$C_{7\beta}$	trans	-	α_D
12	1.473	-12.793	-27.920	-59.539	d	trans	+	α_D	trans	-	α_D	trans	+	α_D
13*	2.741	-11.912	-29.487	-59.868	e	trans	+	α_D	trans	-	α_D	trans	-	α_D
14*	2.873	-11.709	-22.333	-60.072	c	trans	+	α_D	trans	-	α_D	trans	-	$C_{7\beta}$
15*	2.882	-13.260	-23.948	-61.551	f	cis	+	α_D	trans	+	$C_{7\beta}$	trans	-	α_D

*submitted as predictions BWI.a.pdb, BWI.b.pdb, ... , BWI.f.pdb.

Figure S12. Submitted lowest-free energy structures for *N*-aryl trimer 1.

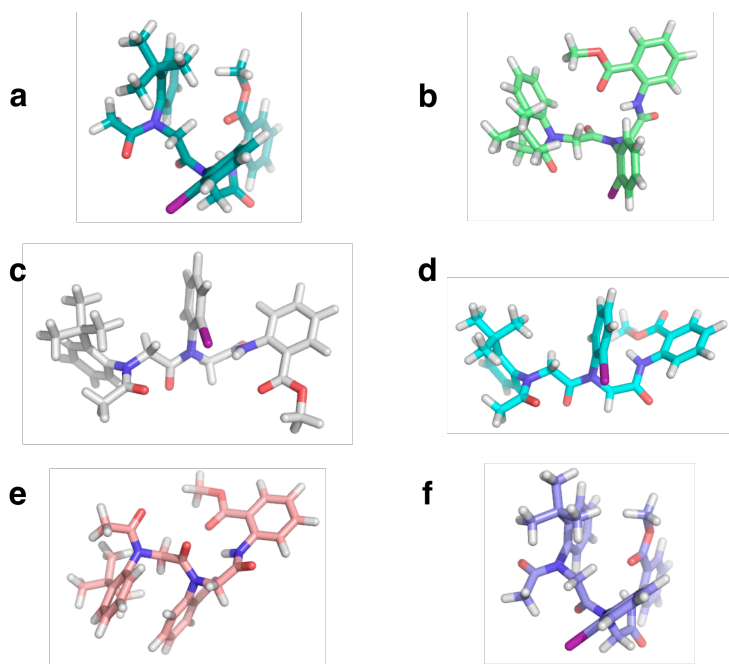


Table S3. Relative QM energies (kcal/mol) and torsion values (degrees) for various HF/3-21G* optimized conformations of peptoid trimer 1.

structure	M052x/ 3-21G*	B3LYP/ 3-21G*	Res1 χ_1	Φ_1	Ψ_1	Res2 χ_1	Φ_2	Ψ_2	ω_3	Res3 χ_3^*
xtal major conformer			98.63	80.37	-168.98	101.35	79.23	4.70	-178.22	-174.26
QM optimization of xtal major conformer	1.34	0.74	96.21	69.35	-169.33	93.23	97.44	-19.86	-175.05	-176.61
minor conformer	0.47	0.65	96.51	63.70	-162.21	-132.52	66.62	12.20	-177.45	-176.49
QM optimizations of REMD snapshots group a state 2	1.14	0.74	96.27	69.38	-169.33	93.23	97.41	-19.88	-175.05	-176.60
group a state 4	1.14	0.74	96.27	69.30	-169.32	93.18	97.45	-19.84	-175.04	-176.60
group a state 6	0.00	0.00	100.89	64.03	-169.19	93.59	97.26	-19.90	-175.15	-176.75
group b state 8	1.14	0.74	96.23	96.34	-169.33	93.13	97.48	-19.90	-175.01	-176.72
group c state 9	7.57	5.29	96.87	80.43	176.15	91.71	-103.15	61.56	-172.69	-168.00
group d state 10	5.43	5.27	105.02	64.07	-161.97	98.33	125.19	-46.00	176.99	2.67
Additional QM optimized conformations C1	8.34	5.58	-96.93	-69.96	170.29	-97.31	-75.26	169.74	177.89	-0.11
C2	5.97	3.11	-96.80	-70.47	170.87	-97.47	-76.09	172.47	179.12	-179.79
C3	9.56	6.47	-96.65	-76.63	179.33	98.02	77.72	-169.22	-178.18	0.33
C4	15.67	14.81	-97.53	-72.38	177.71	92.16	89.14	-175.77	-179.43	-25.76
C5	5.97	3.11	-96.82	-70.47	170.87	-97.47	-76.09	172.47	179.09	-179.81
C6	6.96	3.77	-96.60	-76.78	179.88	98.27	77.95	-170.77	-179.02	-179.97
C7	5.97	3.11	-96.84	-70.84	170.89	-97.47	-76.09	172.47	179.12	-179.79
C8	9.01	6.37	-110.22	68.68	-167.72	98.40	71.59	-168.83	-177.93	0.18
C9	9.64	5.93	85.78	-135.22	-176.06	-95.75	-76.69	171.10	178.87	-179.90
C10	15.34	12.61	-96.56	-69.86	169.62	-98.76	-83.95	-170.11	-2.95	-175.93
C11	11.30	8.14	85.74	-138.12	-171.59	99.89	74.24	-170.53	-178.20	0.22
C12	9.90	7.01	-95.67	-62.40	156.75	124.81	-63.16	166.62	177.21	-0.04
C13	8.34	5.59	-96.91	-70.07	170.34	-97.33	-75.31	169.80	177.91	-0.14
C14	5.97	3.11	-96.82	-70.47	170.85	-97.52	-76.11	172.43	179.12	-179.83
C15	15.78	11.49	84.52	-127.87	-179.32	104.07	-65.03	168.52	178.31	-179.88
C16	15.67	11.89	87.35	-143.68	-150.70	-109.70	63.39	-169.73	-178.43	179.98
C17	8.73	5.48	85.73	-138.07	-171.53	100.06	74.74	-172.29	-179.19	179.90
C18	9.64	5.93	85.83	-135.22	-176.06	-95.66	-76.69	171.10	178.86	-176.94
C19	7.41	4.47	-95.56	-62.64	156.91	124.47	-63.80	169.02	178.18	-179.88
C20	14.89	10.75	-97.37	-81.02	-173.14	-97.21	66.53	-166.33	-178.16	179.96

* = $\angle(\text{C}(\text{Arl})-\text{C}(\text{Arl})-\text{C}(\text{O})-\text{O})$ (O is alkoxy oxygen)

Table S4. The 16 lowest-free energy torsion states for *N*-alkyl trimer 2.

state	ΔG (kcal/mol)	$\langle E \rangle$ (kcal/mol)	Min(E) sampled (kcal/mol)	E after minimization (kcal/mol)	group	ϕ_1	ψ_1	ω_2	ϕ_2	ψ_2	ω_3	ϕ_3	ψ_3	group	mirror- image symmetry (ϕ pattern)
1*	0.000	116.404	53.872	12.333	a	+	α_D	trans	-	α_D	trans	+	C_{7B}	a	+--+
2	0.024	116.390	52.524	16.977	b	+	α_D	trans	+	α_D	trans	+	C_{7B}	b	+++
3*	0.034	116.825	49.059	15.297	c	+	α_D	trans	-	α_D	trans	-	C_{7B}	c	+--
4	0.041	116.846	53.195	16.791	d	-	α_D	trans	+	α_D	trans	+	C_{7B}	d	--+
5*	0.042	116.566	52.323	15.621	b	-	α_D	trans	-	α_D	trans	-	C_{7B}	b	---
6*	0.084	116.478	54.877	14.957	d	+	α_D	trans	+	α_D	trans	-	C_{7B}	d	++-
7	0.093	116.924	54.317	15.967	c	-	α_D	trans	+	α_D	trans	+	C_{7B}	c	-++
8	0.098	116.629	52.856	14.592	a	-	α_D	trans	+	α_D	trans	-	C_{7B}	a	--+
9*	0.244	116.811	53.039	13.801	e	-	α_D	cis	-	α_D	trans	+	C_{7B}	e	--+
10*	0.301	117.020	55.435	14.79	f	+	α_D	cis	+	α_D	trans	+	C_{7B}	f	+++
11	0.309	116.331	53.855	15.326	f	-	α_D	cis	-	α_D	trans	-	C_{7B}	f	---
12	0.354	116.698	51.892	14.834	e	+	α_D	cis	+	α_D	trans	-	C_{7B}	e	++-
13	0.408	117.125	51.213	16.131	g	+	C_{7B}	trans	-	α_D	trans	-	C_{7B}	g	+--
14	0.510	116.362	51.518	16.715	h	+	C_{7B}	trans	-	α_D	trans	+	C_{7B}	h	+++
15	0.539	117.592	52.883	13.712	g	-	C_{7B}	trans	+	α_D	trans	+	C_{7B}	g	-++
16	0.613	116.630	54.025	14.369	i	+	α_D	cis	-	α_D	trans	+	C_{7B}	i	---

*submitted as predictions Npe3.a.pdb, Npe3.b.pdb, ... , Npe3.f.pdb.

Figure S13. Structures of submitted predictions for the *N*-alkyl peptoid trimer 2.

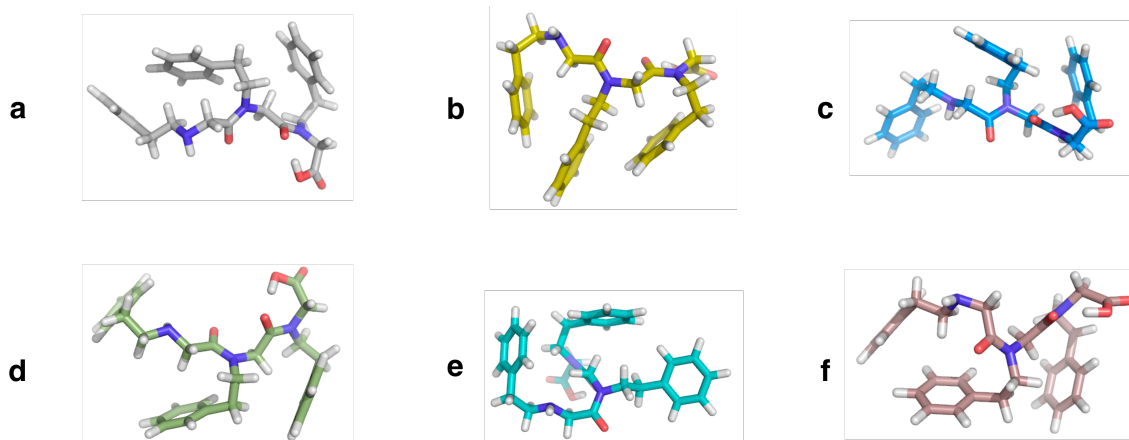


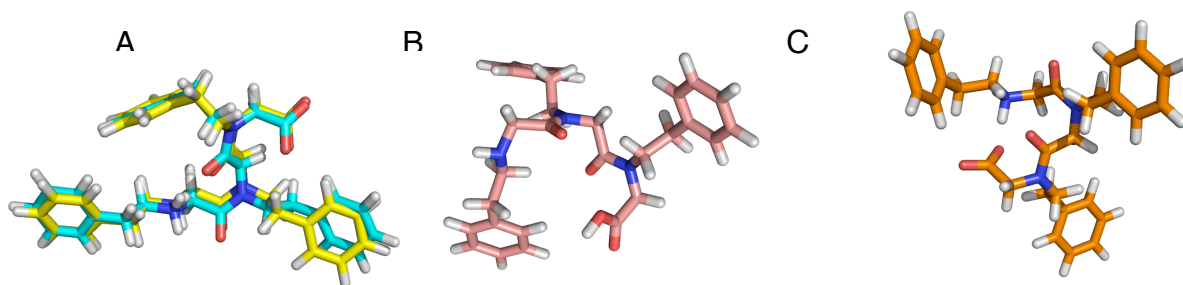
Table S5. QM optimizations of various trimer 2 conformations.

Structures were optimized at HF/6-31G* without water molecules (Xtal 1 and Xtal 2 represent the pair of residue 2 rotamer occupancies found in the crystal, and C1 through C8 are various conformational minima for trimer 2). Relative energies are in kcal/mol and backbone torsions are in degrees.

	B3LYP/ 6-31G*	M052X/ 6-31G*	ψ_1	ω_2	ϕ_2	ψ_2	ω_3	ϕ_3
Xtal 1	14.70	15.97	-120.04	10.63	67.08	156.37	-17.26	-63.73
Xtal 2	13.90	13.39	-120.98	11.86	64.05	160.18	-19.14	-64.07
C1	37.88	38.8	169.16	162.36	79.39	-163.76	135.11	-64.02
C2	41.98	45.05	-177.47	158.00	-69.65	-170.36	-4.19	-69.67
C3	0.00	2.35	114.80	-176.89	75.90	-146.89	-171.67	-71.84
C4	37.87	38.80	169.16	162.34	-79.35	-163.79	135.14	-64.06
C5	0.65	0.00	117.71	-29.89	-53.91	175.59	-164.38	55.35
C6	7.00	7.18	-84.69	135.68	-78.36	-100.74	159.58	-62.55
C7	5.11	4.63	-84.26	148.64	-82.86	-95.25	153.46	-58.96
C8	28.48	28.44	153.94	-12.83	-70.75	-158.74	135.86	-63.03

Figure S14. Selected structures of optimized trimer 2 conformations.

(A) Xtal 1 and 2 overlaid. (B) “C3” (note the C-terminus is protonated). (C) “C5”



Conformational free energy calculations for the cyclic peptoid nonamer

Simulations were initiated from starting conformations modeled after the “threaded-loop” NMR structure of Huang et al. (6). Conformational free energies were computed using MBAR from the eight lowest-temperature (300–490 K) REMD replicas (see Methods for simulation details).

For this prediction target, conformational states were considered to be all possible backbone torsion states defined by ω and ϕ dihedral angles of each peptoid residue (**Figure S3**). For nine peptoid residues with circular symmetry, the number of possible states is $2^{18}/9 = 29127$. In practice, we find that about ~ 1000 of these are actually sampled (note many states may be extremely strained or geometrically impossible).

In earlier work (7), we found that a weak harmonic ϕ -angle restraint would produce backbone conformational propensities closer to QM results by Butterfoss et al. on monomeric Nspe = *N*-(*S*)-(1-phenylethyl glycine) (5). To test this on a larger system of Nspe multimers, we ran an additional set of REMD simulations incorporating this restraint. Consistent with previous findings, the conformational free energies from these simulations favor *cis* amide backbone states slightly more than the unrestrained simulations, and agree less favorably with the QM results (see below), suggesting that the use of restraints may not be appropriate in this context. If we consider the unrestrained and restrained simulations together, the consensus of predicted low-free energy *cis/trans* states include *ccccctttt*, *cccctcct*, *ccccccct*, and *cccctcct* (**Table S6**).

Snapshots of low-energy conformations belonging to each of the lowest-free energy *cis/trans* states were taken from the lowest-temperature simulation replica to be further refined using QM methods. Up to five different dihedral conformations from each *cis/trans* basin (i.e. different sets of ϕ and ψ angles), were used in the selection of these snapshots.

Table S6. Free energies of *cis/trans* states of cyclo-(Nspe)₉, as predicted from restrained and unrestrained REMD simulations.

<i>cis/trans</i> state	Free energy (kcal/mol)	Free energy (w/ restraint) (kcal/mol)
<i>ccccctttt</i>	0	1.482
<i>cccctcct</i>	0.898	1.87
<i>ccccccct</i>	0.905	0
<i>cccttctct</i>	1.098	--
<i>cccctcct</i>	1.134	0.39
<i>cccccttt</i>	1.319	--
<i>cccctcct</i>	1.44	2.77
<i>cccctttt</i>	1.77	--
<i>ccctccct</i>	1.941	2.925

Table S7. The ranked list of (omega-phi) torsional state free energies predicted by (unrestrained) REMD simulation.

The pick1 conformational basin (marked with ****) has a free energy of 1.22 kcal/mol while the conformational basin corresponding to the crystal structure (marked with **) is predicted at ~3.08 kcal/mol.

F (kcal/mol)	cis/trans	phi-state	
0.000	ccccctttt	-+---+--+	
0.562	cccttctct	+---++---	
0.860	ccccctcct	--+---++-	
1.062	ccccctttt	-+---+--+	
1.221	ccctccct	+--+---+---	****
1.301	ccctccctt	+--+---+---	
1.340	ccccccctt	+----+---	
1.395	ccccctttt	-++-+-+--	
1.567	ccctccctt	-+---+--+	
1.568	cccctcctt	+--+---+---	
1.640	ccctcctct	-++-+-+--	
1.786	cctccttct	--+---+--+	
1.944	cccctccct	-++-+-+--	
2.121	ccccctcct	+++---+--	
2.240	cccttcctt	-++-+-+--	
2.251	ccccccctt	--+---+--+	
2.405	ccccctcct	--+++---+	
2.574	ccctccctt	++++-+---	
2.624	cccctcctt	--++-+---	
2.644	ccccccctt	+--+---+---	
2.648	ccccccctt	++++-+---	
2.735	cctccttct	+++---+--	
2.751	ccccctcct	-+--+---+	
2.906	cccctccct	+--+---+---	
2.960	cccctccct	+++---+--	
2.973	cccctcctt	+--+---+---	
3.033	ccccctcct	+++---+--	
3.067	ccccctttt	-+---+--+	
3.078	cccctccct	+--+---+---	**
3.093	cccctcctt	+--+---+---	
3.141	cccctccct	--++-+---	
3.161	ccctccctt	+--+---+---	
...			

***Ab initio* refinement and prediction selection for the cyclic peptoid nonamer**

QM calculations used Gaussian03 and model chemistries and basis sets are indicated in figures and tables (**Tables S3, S5, S8**). A total of 273 conformations were used as starting points for QM calculations. Geometries were optimized at the HF/3-21G* level of theory, and energies were evaluated using DFT functionals B3LYP and M052X.

For our prediction selections, we aimed to pick low-energy conformations while retaining some structural diversity. To aid this, all-atom RMSD-based clustering was performed. Briefly, a *k*-means algorithm was used for initial clustering. Then, a hybrid *k*-medoids algorithm (implemented the MSMBuild2 package (8)) was used to optimize the cluster centers and cluster assignments by minimizing the sum of RMSD distances to each cluster center. The result was 15 clusters, the largest of which had 15 members; five clusters had only a single member. With few exceptions, the conformations cluster into well-defined groups with unique *cis/trans* states and phi-angle assignments (+ or -).

Each cluster was ranked according to the minimum energy of its members. Similar rankings were obtained for the different DFT functionals and basis sets (**Figure S15**). To simplify the presentation, we discuss only the results for B3LYP / 6-311G** and M052X / 6-311G**. For both, the lowest-energy clusters (from 0-3 kcal/mol) all have *ccccccct* states (Figure S3). M052X predicts that the next-highest energy states are *cccccttt* (~3.5–5.0 kcal/mol), while B3LYP predicts that the next-highest energy states are *cccctcct* (~ 3.5 kcal/mol).

The high rankings of *ccccccct* and *cccccttt* by the *ab initio* calculations agree well with the (unrestrained) predictions of replica-exchange molecular dynamics. However, the state *ccccccct* (Figure S4c), predicted as one of the most favorable by REMD, as ranked by *ab initio* methods as one of the least favorable. Keeping this in mind, we chose a diverse set of six structures for our submitted predictions: (1-3) the lowest-energy conformations from each of the three lowest *cccctcct* clusters, (4) the lowest-energy *cccccttt* conformation, (5) the lowest-energy *cccctcct* conformation, and (6) the lowest-energy *ccccccct* conformation. This information is summarized in **Table S9**. Structures from each conformational cluster corresponding to the six predictions are shown in **Figures S16 and S17**.

Table S8. Single-point *ab initio* QM energies of cyclo-(Nspe)₉ conformations selected from REMD simulations, calculated using various model chemistries.

*c/t = cis or trans, +/- = positive or negative phi, m/p = positive or negative chi1

cis/trans	Phi angles	Chi angles	HF/ 3-21G*	B3LYP/ 3-21G*	B3LYP/ 6-31G*	B3LYP/ 6-31G**	B3LYP/ 6- 311G**	M052X / 3- 21G*	M052X / 6- 31G*	M052X/ 6- 31G**	M052X/ 6- 311G**
ccctccct	+--++++-	pmmmmmmp	0.00	0.18	1.47	3.30	2.06	0.00	1.39	0.00	0.00
ccccccct	-+++-----	mmmmmpmm	4.60	4.41	2.74	3.63	5.57	2.86	0.34	0.32	0.90
ccccccct	-+++-----	mmmmmpmm	4.60	4.44	2.40	3.64	5.70	2.94	0.60	0.33	0.93
ccccccct	-+++-----	mmmmmpmm	4.60	4.44	2.43	3.68	4.76	2.30	0.65	0.38	0.98
ccccccct	-+++-----	mmmmppmm	3.79	3.47	2.15	2.60	3.79	2.30	0.84	0.63	1.01
ccccccct	+--++++-	pmmmmmmp	1.38	2.39	0.30	1.21	0.61	3.90	1.71	1.71	1.04
ccccccct	-+++-----	mmmmppmm	3.79	3.47	2.19	2.09	3.82	3.48	0.00	0.66	1.04
ccccccct	+--++++-	pmmmmmmp	3.83	5.09	0.00	0.00	0.08	6.59	2.05	1.68	1.22
ccccccct	+--++++-	pmmmmmmp	4.82	6.96	0.22	1.15	0.00	8.81	1.85	2.23	1.47
ccccccct	-+--+---	mmmmmpmm	4.16	2.21	1.59	2.16	1.90	3.58	2.58	2.47	2.75
ccccccct	--+---+-	mpmmmmmp	12.70	8.80	7.69	8.29	8.71	6.58	3.85	3.50	3.43
ccccccct	--+---+-	mpmmmmmp	12.89	10.54	7.97	8.49	8.61	6.99	4.28	3.08	3.94
cccccttt	-+++-----	mmmmmpmp	8.31	6.22	6.45	6.89	6.92	5.62	4.15	4.20	4.24
cccccttt	-+++-----	mmmmmpmp	7.87	5.47	7.28	7.85	8.52	2.86	4.93	3.57	4.40
cccccttt	--+---+-	mmmmmpmp	10.28	8.92	7.57	8.35	8.69	5.88	5.26	4.30	4.59
ccccccct	+--++++-	pmmmmpmm	2.45	3.77	2.95	3.63	3.12	4.47	4.30	4.24	5.05
cccccttt	--+---+-	mmmmmpmp	5.51	2.83	7.33	8.13	7.46	1.91	5.70	5.15	5.18
ccccccct	+--++++-	pmmmmpmm	2.45	3.78	2.93	3.13	2.98	5.16	4.99	3.85	5.18
cccccttt	--+---+-	mmmmmpmp	5.51	2.83	6.46	8.14	7.47	1.91	5.54	5.16	5.19
ccccccct	--+---+-	mpmmmpmp	13.47	8.98	8.55	8.99	9.35	6.79	5.42	5.28	5.20
cccccttt	--+---+-	mmmmmpmp	5.51	2.83	7.36	8.17	7.50	1.94	5.20	5.18	5.23
ccccccct	+--++++-	pmmmppmm	4.20	1.35	2.69	3.34	2.99	4.93	5.75	5.17	5.32
ccccccct	-+--+---	mmmmmpmm	12.11	6.90	7.99	8.64	9.05	6.46	6.01	5.85	5.45
ccccccct	++-+-----	mpmmmmmp	1.44	0.00	2.37	3.12	1.51	3.45	6.08	6.18	5.57
ccccccct	+--++++-	mmmmmpmp	10.58	6.76	6.05	6.77	6.30	7.96	6.83	6.14	5.73
ccccccct	-+--+---	mmmmmpmm	12.11	6.90	7.98	8.64	8.30	6.46	6.02	5.77	5.75
cccccttt	-+++-----	mpmmmpmp	6.08	3.59	7.27	7.73	8.08	3.06	5.40	4.69	5.81
ccccccct	--+---+-	mpmmmpmp	15.47	11.06	9.70	10.18	11.09	7.94	6.16	5.49	5.82
cccccttt	-+++-----	mpmmppmp	8.94	5.71	7.82	8.10	9.36	5.42	5.23	5.01	6.26
ccccccct	--+---+-	mpmmmpmp	12.84	7.80	9.01	9.57	10.78	5.87	6.11	6.24	6.98
ccccccct	++-+-----	mpmmmmmp	3.09	1.73	3.09	3.92	2.61	5.97	6.13	7.01	7.03
cccccttt	-+++-----	mpmmpppp	7.45	3.82	9.65	9.94	10.48	1.66	6.44	6.21	7.22
ccccccct	-+++-----	mmmmmpmp	17.41	12.89	11.45	12.87	13.78	7.04	6.67	6.45	7.25
ccccccct	+--++++-	pmmmppmp	7.55	5.52	4.00	5.32	4.49	9.99	7.95	8.76	7.36
ccccccct	--+---+-	mmmmmpmp	10.11	6.98	6.80	7.49	7.03	8.34	8.55	8.38	7.60
ccccccct	+-----+	mmmmmpmm	16.10	9.70	9.55	10.12	9.86	9.07	8.36	7.75	7.95
ccccccct	-+--+---	mmmmmpmp	14.53	12.78	10.32	10.99	10.66	11.07	8.10	7.72	7.99
ccccccct	+-----+	mmmmmpmm	16.93	11.54	10.72	11.40	11.33	10.42	8.23	7.89	8.12
cccccttt	-+++-----	mmmmpppp	11.75	9.89	12.26	12.06	13.16	7.18	7.85	7.30	8.14
ccccccct	--+---+-	mpmmmmmp	15.12	10.97	8.68	10.13	9.86	11.55	8.52	8.30	8.23
ccccccct	+-----+	pmmmmpmm	14.86	10.22	9.49	10.12	9.90	10.37	8.56	8.47	8.28

ccccccct	--++-+--+	nnnnppmmp	9.63	6.38	6.99	7.65	7.35	8.73	8.29	8.36	8.30
ccccctttt	-+---+---	nnppmnnppp	7.05	3.55	9.89	10.39	10.60	1.84	7.80	6.76	8.35
ccccccct	-+++--+++	nnppmppmmp	16.64	12.21	12.37	12.78	14.06	9.14	8.16	7.67	8.35
ccccctttt	-+++--+---	nnnnnnpppp	13.55	10.98	9.85	10.24	9.90	11.57	8.88	8.53	8.39
ccccccct	+-----+---	ppnnmppmnn	14.04	9.67	9.67	10.45	9.63	11.59	9.41	9.05	8.52
ccccccct	+--+--+---	nnnnnnppmnn	20.11	13.32	13.84	14.55	14.13	10.46	9.53	9.24	8.55
ccccctttt	-+++--+---	nnnnnnpppp	12.51	9.88	10.15	10.63	11.37	9.87	8.88	8.80	8.95
ccccctttt	-+++--+---	nnppmnnppp	11.12	7.52	11.68	12.26	12.26	5.77	8.98	7.97	8.99
ccccccct	+-----+---	nnnnnnppmnn	14.98	9.50	8.39	10.58	10.83	9.80	9.35	9.15	9.15
ccccccct	+-----+---	nnnnnnppmnn	14.98	9.50	9.81	10.57	10.61	10.23	9.42	8.92	9.16
ctctctct	---+---++	nnppnnnnnn	11.72	8.34	6.11	7.14	6.27	12.19	9.78	8.96	9.19
ccccccct	+-----+---	nnnnnnppmnn	14.98	9.50	9.81	10.58	9.88	9.57	9.54	9.22	9.19
ccccccct	+-----+---	ppnnmppmmp	13.42	7.04	9.09	10.02	10.02	8.28	9.70	8.79	9.21
ctctctct	---+---++	nnppnnnnnn	11.73	8.33	5.74	7.16	6.24	11.85	9.76	9.41	9.25
ccccccct	++-----+---	ppnnnnnnnn	9.07	6.13	7.80	8.78	7.22	9.20	9.98	9.87	9.31
ccccctttt	-+++--+---	nnnnpppppp	16.84	12.46	13.08	13.78	13.99	10.73	10.07	10.30	9.45
ctctctct	---+---++	nnppnnnnnn	12.05	6.76	6.46	6.73	6.09	10.60	9.73	10.53	9.66
ccccccct	++-----+---	ppnnmppmnn	9.32	6.61	7.74	8.42	7.36	10.03	9.73	9.76	9.85
ccccccct	-+++--+---	nnppppmmp	17.51	12.43	13.34	13.87	13.76	10.56	10.65	9.90	9.90
ctctctct	+-----+---	ppmppmppm	10.17	8.01	7.69	8.43	7.01	13.26	11.24	11.35	10.22
ccccctttt	-+++--+---	nnnnnnpppp	14.30	12.24	10.99	11.67	10.57	14.52	11.23	11.02	10.52
ccccccct	+-----+---	nnnnnnppmnn	17.97	12.35	10.02	10.62	10.02	14.77	11.35	10.83	10.64
ctctctct	+-----+---	nnppppmnn	9.41	7.26	7.36	8.10	7.32	12.97	10.90	10.91	10.66
ccccccct	+-----+---	nnppmppmnn	20.25	14.81	11.69	12.47	11.99	16.57	11.35	10.77	10.79
ccccccct	-++++-----	nnnnpppppp	14.81	13.05	10.38	9.55	12.39	11.70	9.14	9.16	10.99
ctctctct	-+++--+---	ppmppmppm	12.84	6.58	11.91	12.08	13.04	7.45	10.99	10.14	11.23
ccccccct	++-----+---	ppnnnnnnpp	9.83	6.07	8.73	9.64	8.38	9.61	11.49	11.54	11.36
ccccccct	+-----+---	nnnnnnppmnn	16.76	11.07	9.52	10.41	9.53	13.00	11.81	11.66	11.60
ccccccct	+--+--+---	nnppmppmnn	19.34	14.53	11.11	11.75	11.44	17.36	12.42	12.11	11.63
ccccctttt	-+++--+---	nnnnnnpppp	14.67	12.24	14.09	14.30	13.81	11.04	11.66	11.17	11.68
ccccccct	-++++-+--+	nnnnpppppp	21.13	19.49	11.45	12.15	11.86	20.42	12.39	12.35	11.71
ccccccct	-+++--+---	nnppppmmp	17.64	13.67	13.37	13.80	13.51	14.07	13.06	12.06	11.96
ccccccct	+-----+---	nnppmppmnn	19.28	14.26	12.10	12.59	11.83	15.73	12.52	12.15	11.97
ccccccct	+--+--+---	ppnnmppmmp	7.10	3.18	6.39	7.58	7.17	8.90	12.51	11.57	11.99
ctctctct	++-----+---	ppnnppmnn	14.15	9.24	10.99	11.43	10.23	11.91	12.71	12.39	12.09
ccccccct	++-----+---	ppnnnnnnpp	11.13	7.34	8.80	9.96	9.22	11.28	11.79	11.90	12.29
ccccctttt	-+++--+---	nnnnnnpppp	16.60	12.83	13.30	12.79	14.25	13.17	12.66	12.28	12.87
ctctctct	--+---+--+	nnnnnnppmmp	13.70	11.35	10.85	11.90	10.86	15.90	14.16	14.14	13.85
ccccctttt	-+++--+---	nnppppppp	17.78	12.19	16.34	16.97	18.34	10.77	14.14	13.06	13.86
ccccctttt	-+++--+---	nnnnnnpppp	16.21	13.26	14.64	15.11	15.20	13.22	13.48	13.33	14.05
ccccctttt	-+++--+---	nnppppppp	17.78	12.19	15.26	16.98	17.71	11.32	14.15	13.26	14.10
ctctctct	+-----+---	nnppppmnn	13.52	16.12	7.69	8.55	6.53	22.90	14.20	14.20	14.14
ccccctttt	-+++--+---	nnnnnnpppp	19.33	13.86	16.41	16.98	17.94	12.58	14.46	14.08	14.89
ctctctct	+-----+---	nnppppmnn	16.13	17.99	10.15	10.94	8.97	25.02	16.16	15.97	16.09
ctctctct	--+---+--+	ppmppmppp	24.13	21.36	14.92	15.63	15.22	20.83	16.34	16.02	16.18
ctctctct	+-----+---	nnppppmnn	16.13	18.00	10.19	10.65	9.04	24.03	16.23	16.80	16.20

Figure S15. Conformational clusters of cyclo-(Nspe)₉, ranked by (top) B3LYP/6-31G*** and (bottom) M05-2X/6-311G**.

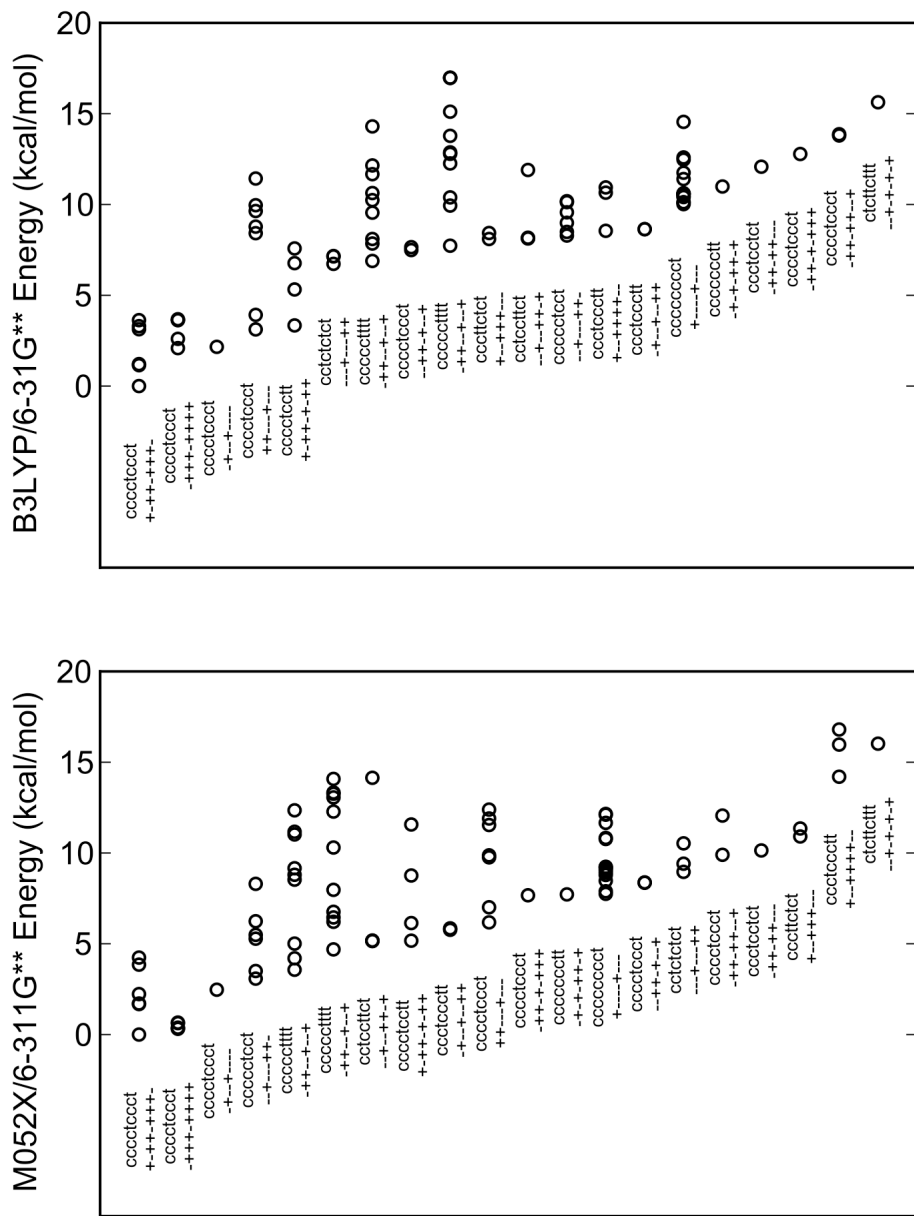


Table S9. A summary of the backbone structures of submitted structure predictions for cyclo-(Nspe)₉.

Rank	<i>cis/trans</i> state	Phi-angle state
1	<i>ccccccct</i>	+--+--++++-
2	<i>ccccccct</i>	-++++-++++
3	<i>ccccccct</i>	--+---+-----
4	<i>cccccttt</i>	-++--+-+--+
5	<i>ccccctct</i>	+--+--+-+--+
6	<i>ccccccct</i>	+-----+-----

Figure S16. Conformational clusters corresponding to the three lowest-energy *ccccccct* states.

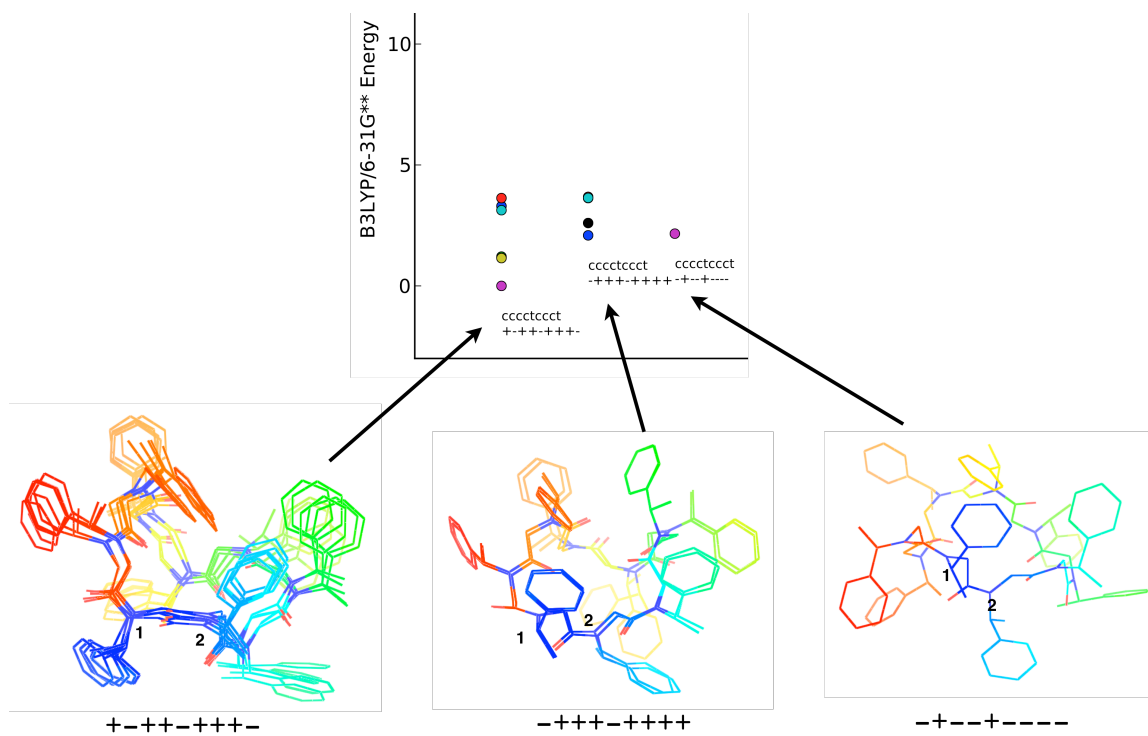
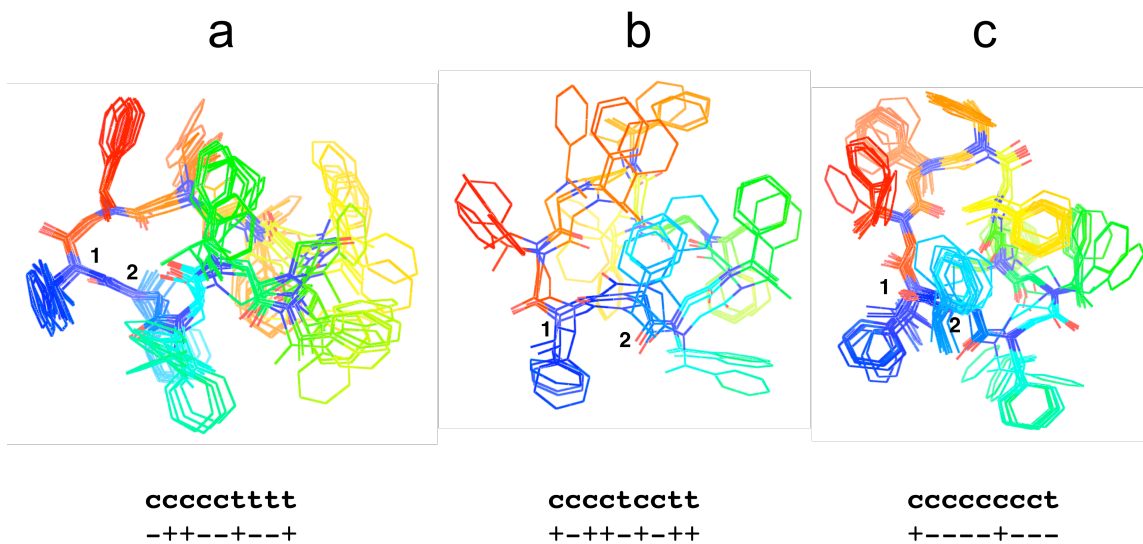


Figure S17. Conformational clusters corresponding to the lowest-energy states for states (a) *ccccctttt* (b) *cccctcctt* and (c) *ccccccct*.



QM calculations comparing experimental and predicted structures

Evaluation of the relative energies of the pick1 and the crystal structure with no ethanol shows that the two density functionals used here disagree on which is more favorable. B3LYP finds the optimized crystal conformation to be the lowest energy of all 273 cyclo-(Nspe)₉ conformations tested (and ~2 kcal/mol lower than pick1), while M05-2X predicts pick1 to be the lowest energy sampled conformation and ~3 kcal/mol more favorable than the crystal.

Table S10. Relative energies (kcal/mol) of cyclo-(Nspe)₉ after optimization at HF/3-21G* without ethanol

	B3LYP/ 6-311G**	M052X/ 6-311G**
xtal	0.00	2.93
pick1	2.06	0.00

We can further explore the inherent stability these conformations by (1) removing side chains and (2) considering the effects of interactions with solvent molecules:

What are the effects of Nspe side chains?

To probe the importance of side chains in determining cyclo-(Nspe)₉ backbone preferences, we performed additional DFT calculations on cyclo-(Sar)₉ analogs (Sar = *N*-methyl glycine) of all 273 structures. Both B3LYP and M05-2X functionals predict that the pick1 backbone conformation is more stable. This preference is again more pronounced in M05-2X, which may be due to the more compact structure of pick1 being favored by the dispersion interactions, which are better represented in M05-2X.

Table S11. Relative energies (kcal/mol) of cyclo-(Sar)₉ after optimization at HF/3-21G* without ethanol

	B3LYP/ 6-311G**	M052X/ 6-311G**
xtal	1.06	3.82
pick1	0.00	0.00

What is the effect of ethanol?

The cyclo-(Nspe)₉ is crystalized with an ordered solvent ethanol molecule which form a hydrogen bond with a backbone carbonyl oxygen. An ethanol cannot fit in the same orientation with the pick1 conformation due to clashes with side chain atoms. However the effect of this ethanol on the peptoid structure can be approximated with the cyclo-(Sar)₉ models.

Optimization of cyclo-(Nspe)₉ versions of the crystal backbone and pick1 including the complexed ethanol gives a lower energy for the crystal conformation at both B3LYP and M05-2X levels of theory (below, left columns). However when the energies of these same backbone conformations are recalculated without the ethanol (and no additional minimization), the crystal geometry remains slightly lower at the B3LYP level of theory but pick1 is predicted to be more favorable at M05-2X.

As M052X better represents dispersion forces, it may be that at interactions with the complexed ethanol helps to stabilize the crystal conformation relative to pick1.

Table S12. Relative energies (kcal/mol) of cyclo-(Sar)₉ after optimization at HF/3-21G* with ethanol. Energies are then calculated with (+) or without (-) the ethanol

	B3LYP/ 6-311G**	M052X/ 6-311G**		B3LYP/ 6-311G**	M052X/ 6-311G**
xtal+EtOH	0.00	0.00	xtal-EtOH	0.00	1.14
pick1+EtOH	2.16	1.73	pick1-EtOH	0.86	0.00

Table S13. RMSD of optimized structures in this section, compared to the experimental crystal structure using backbone C α , N, C, and O:

Structure	RMSD (\AA)*
xtal+EtOH (Nspe)	0.237
xtal-EtOH (Nspe)	0.227
xtal+EtOH (Sar)	0.340
xtal-EtOH (Sar)	0.751
pick1 (Nspe)	1.003
pick1+EtOH (Sar)	1.219
pick1-EtOH (Sar)	1.401

References

1. Winkler FK & Dunitz JD (1971) The non-planar amide group. *J. Mol. Biol.* 59(1):169–182.
2. Shell MS, Ozkan SB, Voelz V, Wu GA, & Dill KA (2009) Blind Test of Physics-Based Prediction of Protein Structures. *Biophysical Journal* 96(3):917–924.
3. Ozkan SB, Wu GA, Chodera JD, & Dill KA (2007) Protein folding by zipping and assembly. *Proceedings of the National Academy of Sciences of the United States of America* 104(29):11987.
4. Shirts MR & Chodera JD (2008) Statistically optimal analysis of samples from multiple equilibrium states. *The Journal of Chemical Physics* 129(12):124105.
5. Butterfoss GL, Renfrew PD, Kuhlman B, Kirshenbaum K, & Bonneau R (2009) A Preliminary Survey of the Peptoid Folding Landscape. *Journal of the American Chemical Society* 131(46):16798-16807.
6. Huang K, *et al.* (2006) A Threaded Loop Conformation Adopted by a Family of Peptoid Nonamers. *Journal of the American Chemical Society* 128(5):1733-1738.
7. Voelz VA, Dill KA, & Chorny I (2010) Peptoid conformational free energy landscapes from implicit-solvent molecular simulations in AMBER. *Biopolymers* 96(5):639-650.
8. Beauchamp KA, *et al.* (2011) MSMBuild2: Modeling Conformational Dynamics on the Picosecond to Millisecond Scale. *Journal of Chemical Theory and Computation* 7(10):3412–3419.